EUROPEAN JOURNAL OF COMPUTATIONAL MECHANICS, 2017
VOL. 26, NO. 3, 309–335
https://doi.org/10.1080/17797179.2017.1354578

Direct computation of stress intensity factors in finite element method

J. Caicedo and A. Portela

Faculty of Technology, Department of Civil Engineering, University of Brasília, Brasília, Brazil

ABSTRACT

This paper is concerned with the direct computation of stress intensity factors (SIFs) in the finite element analysis of the mixed-mode deformation of homogeneous cracked plates. The direct computation of SIFs is a natural consequence of a regularisation procedure, introduced before the finite element analysis takes place that uses a singular particular solution of the crack problem to introduce the SIFs as additional problem primary unknowns. In this paper, the singular term of Williams' eigenexpansion, derived for a semi-infinite crack, is used to regularise the elastic field of an edge-cracked finite plate. Two cracked plates were analysed with this technique, in order to assess the accuracy and efficiency of the formulation. The results obtained in this work are in perfect agreement with those obtained with the dual boundary element method and other published results. The accuracy and efficiency of the implementation described herein make this a reliable and robust formulation, ideal for the study of crack-growth problems, with the finite element method.

ARTICLE HISTORY
Received 8 April 2017
Accepted 10 July 2017

KEYWORDS
FEM; stress intensity factor; singularity subtraction regularisation; crack tip elastic field; Williams' singular solution; cracked plates

1. Introduction

Within the limits of linear elastic analysis, the stress field is unbounded at the tip of a crack. This was early reported by Brahtz (1933) and later by Williams (1952) who, after an investigation of the analytical form of these singularities demonstrated that under all possible combinations of boundary conditions, the stress becomes infinite at the tip of a crack. From a physical point of view, unbounded elastic fields are meaningless. Nevertheless, unbounded stresses cannot be ignored as their presence indicates that new phenomena (e.g. plasticity, fracture, etc.) may occur, leading to localised damage in practical situations. In this paper, the term *singularity* is used to denote the cases in which the elastic stress field becomes unbounded. If r denotes the distance measured from the crack tip, the stress field is of the order $r^{-1/2}$ which becomes singular as r tends to zero. The stress intensity factor (SIF), defined at the crack tip, is a measure of the strength of this singularity.

CONTACT A. Portela aportela@unb.br

The presence of the stress singularity in the numerical model raises considerable numerical difficulties by virtue of the need of simultaneously representing both the singular and the finite stresses in the numerical model. The most important approaches that have been devised to overcome this difficulty, in the standard finite element method (FEM), in the extended finite element method (XFEM), in the boundary element method (BEM) and in mesh-free methods, are briefly reviewed in the following.

The use of quarter-point isoparametric finite elements, introduced by Barsoum (1976) and Henshell and Shaw (1975), suggested the application of quarter-point boundary elements at the crack tip, as an alternative to the mesh refinement procedure. However, while quarter-point finite elements both represent the $r^{1/2}$ displacement behaviour and introduce a $r^{-1/2}$ singularity in the stress field, the use of quarter-point elements in the BEM, in which displacements and tractions are approximated independently, enables only the displacement behaviour to be properly represented. This feature was early noticed by Cruse and Wilson (1977), who introduced traction-singular quarter-point boundary elements for the correct representation of the singularity in the stress field. SIFs can be computed from quarter-point elements by the displacement correlation procedure. The application of this procedure over quarter-point elements, first presented by Blandford, Ingraffea, and Liggett (1981), was called a two-point formula by Smith and Mason (1987). The computation of SIFs from traction-singular quarter-point boundary elements was presented by Martinez and Dominguez (1984).

While the above methods represent the stress singularity in the numerical model, an alternative approach, developed by Symm (1963) in potential theory, is based on the subtraction of this singularity from the numerical model. In fracture mechanics applications, the singularity subtraction technique is a procedure that uses a singular particular solution of the crack problem to regularise the stress field and to introduce, simultaneously, the SIFs as additional primary unknowns in the problem. This approach was first applied by Xanthis, Bernal, and Atkinson (1981) for anti-plane problems and by Aliabadi, Rooke, and Cartwright (1987) to solve symmetrical crack problems using the BEM.

In the case of non-symmetrical problems, the singular tractions are not among the boundary element unknowns and consequently, there is no singularity in the numerical model to be subtracted. The application of the sub-regions BEM is an obvious way to circumvent this difficulty, as shown by Aliabadi (1987). However, artificial boundaries introduced by this method are not strictly necessary in the analysis of a crack problem. An alternative strategy, developed by Portela, Aliabadi, and Rooke (1991), first introduces the stress equations of an internal point, approaching the crack tip, as primary unknowns in the boundary element formulation. Then, the stress field, singular at this internal point, can now be regularised with the singularity subtraction technique. The extension of this singularity subtraction technique to pure opening mode analysis of sharp notches was first reported by Portela, Aliabadi, and Rooke (1989).

Alternatively, the evaluation of SIFs can be based on contour integrals which are path-independent. The J-integral has been used quite effectively in the dual BEM, as a post-processing technique, for the evaluation of SIFs by Portela, Aliabadi, and Rooke (1992). A simple procedure, based on the decomposition of the elastic field into its respective symmetric and anti-symmetric mode components, is used to decouple the SIFs of a mixed-mode problem. Although this technique does not perform a regularisation of the elastic field with the crack tip singularity subtraction, it is very accurate because it uses the elastic field computed at internal points which is a highly accurate operation in the BEM due to the fundamental solutions.

As an alternative to the J-integral post-processing technique, the direct computation of the SIFs, as additional primary unknowns in the dual BEM, was first presented by Portela, Aliabadi, and Rooke (1992). In order to avoid numerical difficulties that arise from the presence of a singularity in the numerical model, it is convenient to subtract this singularity from the original problem, before it is solved by the numerical method. This regularisation considers a singular particular solution of the problem and forces the original elastic field to be identical to this particular solution, at the singular point. By virtue of the analytical structure of the singular particular solution that represents the crack tip elastic field, the modified problem includes the SIFs as additional primary unknowns. Finally, the numerical method can be easily applied to solve the modified problem which is now regular and consequently can lead to highly accurate solutions simply with coarse meshes.

In the standard FEM, the hybrid crack tip element (HCE), see Tong, Pian, and Lasry (1973), can be used for the direct computation of SIFs, as reported by Karihaloo and Xiao (2001) and Xiao, Karihaloo, and Liu (2004). The HCE represents a crack by only one super-element which includes the crack tip and is connected compatible with the surrounding finite elements. The HCE uses a truncated asymptotic crack tip displacement and stress expansions. It is important to stress that, while HCE makes the numerical modelling of the elastic field with the crack tip singularity included, the formulation presented in this paper completely removes the singularity before the finite-element analysis of the regularised elastic field with no convergence difficulties and highly accurate results.

Mesh-free methods, see Belytschko, Krongauz, and Organ (1996), have received much attention recently, since they eliminate the need for a discretisation mesh and hence, they appear to demonstrate significant potential to the moving boundary problem inherent in crack-growth processes. Comprehensive reviews of mesh-free methods can be found in Li and Liu (2002), Liu and Gu (2005), and Nguyen, Rabczuk, Bordas, and Duflotd (2008). In these methods, the moving least squares approximation is possibly the most used method to interpolate discrete data with a good accuracy. The order of continuity of the approximation can be set to a desired value, as reported by Sladek, Sladek, Wunsche, and Zhang (2009). The treatment of crack discontinuities, the main issue of modern mesh-free methods, has been modelled in different ways; Carpinteri, Ferro, and Ventura (2003) used a virtual extension of the crack in the direction of the tangent at the crack tip, while Wen and Aliabadi (2007) considered enriched basis functions in the moving least squares interpolation. Enriched weight/basis functions, by incorporating *apriori* knowledge of the solution that is a jump function along the discontinuity and the asymptotic crack tip displacement field, have been successfully applied to fracture problems, as reported by Fleming, Chu, Moran, and Belytschko (1997), Gu & Zhang (2008) and Lu, Belytschko, and Tabbara (1995). However, the main difficulty of this strategy is that the enrichment area must be limited, when multiple cracks are densely distributed or when crack tips are close to the boundaries which is a drawback of this new generation mesh-free methods. A new approach was presented by Rabczuk and Belytschko (2007), in which no representation of the crack topology is needed. In this context it is worth of mention the work of Bordas, Rabczuk, and Zi (2008), in which only an extrinsic discontinuous enrichment and no near-tip enrichment is required.

Semi-analytical formulations, in which the singular and finite stress fields can be represented more accurately, play an important role in the treatment of crack problems. This is the case of the scaled boundary FEM, presented by Natarajana, Ooi, Chiong, and Song (2014), Natarajana, Songa, and Belouettarb (2014), and Ooi, Song, Loi, and Yang (2012) that does not require special numerical integration technique, does not require a priori knowledge of the asymptotic fields and the stiffness of the region containing the crack tip is computed directly.

The XFEM, developed by Belytschko and Black (1999), is a modern numerical modelling tool that offers great flexibility in the analysis of the fracture process. The theory and applications of XFEM, in the linear and non-linear problems of continua and structures were presented by Khoei (2015). The XFEM enriches the local standard finite-element approximation space to incorporate *apriori* knowledge of the solution, with a displacement discontinuity function across the crack and the asymptotic solution at nodes surrounding the crack tips, with the use of the partition of unity method (PUM), (see Melenk and Babuska, 1996). As a result, the numerical model consists of three types of finite elements: non-enriched elements, fully enriched elements and partially enriched elements, the so-called *blending* elements. By virtue of the enrichment process, the XFEM overcomes the need of using finite-element meshes conforming with the crack discontinuity, as well as the adaptive remeshing as the crack grows, as is the case with the standard FEM. The XFEM considerably facilitates the meshing operations in the solution of complex structures, in the sense that it does not require the finite element mesh (FEM) to conform to the crack faces, (see Hedayati and Vahedi, 2014). The solution accuracy of the local fields around crack tips is a direct consequence of the choice carried out for the enrichment functions which define *apriori* knowledge of the solution. Alternative crack tip enrichment techniques have been devised to simulate failure and yet allow for direct estimation of the SIFs. In this regard, Liu, Xiao, and Karihaloo (2004) introduced a method which is still relying on the PUM, but with specific enrichment functions that are the Williams' series. An efficient enrichment strategy was presented by Akhondzadeh, Khoei, and Broumand (2017), for modelling crack tips terminating at a bi-material interface within the XFEM framework.

Error estimation for the discretisation error in XFEM calculations for cracks is a very important subject. Reference work in this area was presented by Bordas and Duflot (2007), Bordas, Duflot, and Le (2008), Duflot & Bordas (2008), Estrada et al. (2012), Prange, Loehnert, and Wriggers (2012), Rdenas, Estrada, Tarancn, and Fuenmayor (2008), and Rodenas, Estrada, Diez, and Fuenmayor (2010).

An evaluation of the performances of BEM-based methods and their comparison with XFEM, in modelling cracked structures undergoing fatigue crack-growth, was carried out by Dong and Atluri (2013). After a thorough examination of a large set of numerical examples of varying degrees of complexity these researchers concluded that the BEM-based methods are far more accurate than XFEM for computing SIFs and thus the fatigue-crack-growth-rates; they also require minimal effort for modelling the non-collinear propagation of cracks under fatigue, without using the Level Set or Fast Marching methods to track the crack surface and finally, they can easily perform fracture and fatigue analysis of complex structures, such as repaired cracked structures with composite patches and damage in heterogeneous materials.

In contrast with the dual BEM, the regularisation of the crack tip elastic field, to compute the SIFs in the FEM, has not received much attention, to the author's knowledge. Indeed, the different methods that have been developed in FEM, XFEM and mesh-free methods share a common feature that regards the well-known difficulties that arise in the numerical modelling of elastic fields with singularities. Hence, there is a clear need of research in the field of this paper, in order to develop new robust and efficient numerical methods for the finite element analysis of these problems.

This paper is concerned with the direct computation of SIFs through the singularity subtraction technique in the FEM, to provide an efficient and accurate way of analysing the mixed-mode deformation of homogeneous cracked plates. The organisation of the paper is as follows. In Section 2, the original elastic field of a cracked plate is presented. The regularisation of the original elastic field, with the singularity subtraction technique is presented in Section 3. Section 4 presents the singular particular solution of the elastic field used in the regularisation process which is the first term of Williams' eigenexpansion. The singularity subtraction technique is presented for the two-dimensional finite element analysis of homogeneous elastic cracked plates, in Section 5. In Section 6, some numerical results are presented illustrating the effectiveness and robustness of the present regularisation process that, through the singularity subtraction technique, allows to the direct computation of the SIFs in the FEM. Finally, concluding remarks are presented in Section 7.

2. Original elastic field

Consider a two-dimensional cracked plate with domain Ω and boundary $\Gamma = \Gamma_u \cup \Gamma_t$. In the absence of body forces, the elastic field satisfies the equations

$$\mathbf{L}^T \sigma = 0 \tag{1}$$

$$\varepsilon = \mathbf{L}\,\mathbf{u} \tag{2}$$

$$\sigma = \mathbf{D}\,\varepsilon \tag{3}$$

in domain Ω, with boundary conditions

$$\mathbf{u} = \bar{\mathbf{u}} \quad \text{on boundary} \quad \Gamma_u \tag{4}$$

and

$$\mathbf{t} = \mathbf{n}\,\sigma = \bar{\mathbf{t}} \quad \text{on boundary} \quad \Gamma_t, \tag{5}$$

in which the vectors σ and ε represent respectively the stress and the strain components; $\mathbf{D}$ is the matrix of the elastic constants; $\mathbf{L}$ is a matrix differential operator; the vectors $\mathbf{u}$ and $\mathbf{t}$ represent respectively the displacement and the traction components; $\bar{\mathbf{u}}$ and $\bar{\mathbf{t}}$ represent prescribed values respectively of the displacements and tractions and $\mathbf{n}$ represents the outward unit normal components to the boundary.

3. Regularised elastic field

Because of convergence difficulties that arise in numerical modelling of elastostatic problems with singular fields, an alternative technique involving the subtraction of the singularity can be used. Before presenting this technique which introduces the SIFs as additional primary unknowns in the problem, some basic definitions will be presented, concerning singular elastic fields.

In this paper, a singular elastic field is defined as one with unbounded stresses at one point in the problem domain, but with displacements bounded everywhere. In contrast, a regular elastic field has both the stress and the displacement fields bounded at every point in the problem domain.

It is well known that the stress field is singular in the neighbourhood of a crack tip. Hence, in order to avoid numerical difficulties arising from the presence of a singularity in the stress field, it is convenient to modify the original problem before it is solved by the FEM. Under the assumption of linear behaviour, where the principle of superposition is valid, the elastic field can be decomposed into a regular (R) and a singular (S) part as follows:

$$\sigma_{ij} = (\sigma_{ij} - \sigma_{ij}^S) + \sigma_{ij}^S = \sigma_{ij}^R + \sigma_{ij}^S \tag{6}$$

and

$$u_i = (u_i - u_i^S) + u_i^S = u_i^R + u_i^S, \tag{7}$$

where $\sigma_{ij}^R = \sigma_{ij} - \sigma_{ij}^S$ and $u_i^R = u_i - u_i^S$ are the regular components, respectively, of the stress and displacement fields of the original problem; σ_{ij}^S and u_i^S are respectively the stress and displacement components of a particular solution of the original problem, representing the singular elastic field. If appropriate functions are chosen for this particular singular field, then Equations (6) and (7) completely regularise the original problem, in the sense that the stress components σ are now non-singular.

As a consequence of this regularisation, the analysis of the elastic problem can now be carried out on the regular elastic field only, represented by components σ_{ij}^R and u_i^R; the components σ_{ij}^S and u_i^S of the singular field automatically satisfy identically the field equations, because they are defined as a particular solution of the original problem. Hence, the elasticity Equations (1)–(3) can now be written as

$$\mathbf{L}^T \sigma^R = 0 \tag{8}$$
$$\varepsilon^R = \mathbf{L}\,\mathbf{u}^R \tag{9}$$
$$\sigma^R = \mathbf{D}\,\varepsilon^R \tag{10}$$

in domain Ω, with boundary conditions

$$\mathbf{u}^R = \bar{\mathbf{u}} - \mathbf{u}^S \quad \text{on boundary} \quad \Gamma_u \tag{11}$$

and

$$\mathbf{t}^R = \bar{\mathbf{t}} - \mathbf{t}^S \quad \text{on boundary} \quad \Gamma_t. \tag{12}$$

It is important to note that this regularised elastic field is governed by the same equations of the original field, except for the boundary conditions (11) and (12) where additional terms, respectively, $\mathbf{u}^S$ and $\mathbf{t}^S$ are now included. These additional terms, components of a particular solution of the original problem, represent the singular elastic field.

4. William's singular particular solution

The particular solution used in Equations (6) and (7), denoted by components σ_{ij}^S and u_i^S, represents the singular elastic field in the neighbourhood of the crack tip. It can be considered through the first term of the eigenexpansion derived by Williams (1952), for a semi-infinite edge crack. The stress components are given by

$$\sigma_{11}^S = \frac{K_I}{\sqrt{2\pi r}} \cos\frac{\theta}{2}\left(1 - \sin\frac{\theta}{2}\sin\frac{3\theta}{2}\right) + \frac{K_{II}}{\sqrt{2\pi r}} \sin\frac{\theta}{2}\left(2 + \cos\frac{\theta}{2}\cos\frac{3\theta}{2}\right), \tag{13}$$

$$\sigma_{22}^S = \frac{K_I}{\sqrt{2\pi r}} \cos\frac{\theta}{2}\left(1 + \sin\frac{\theta}{2}\sin\frac{3\theta}{2}\right) - \frac{K_{II}}{\sqrt{2\pi r}} \sin\frac{\theta}{2}\cos\frac{\theta}{2}\cos\frac{3\theta}{2} \tag{14}$$

and

$$\sigma_{12}^S = \frac{K_I}{\sqrt{2\pi r}} \cos\frac{\theta}{2}\sin\frac{\theta}{2}\cos\frac{3\theta}{2} + \frac{K_{II}}{\sqrt{2\pi r}} \cos\frac{\theta}{2}\left(1 - \sin\frac{\theta}{2}\sin\frac{3\theta}{2}\right) \tag{15}$$

and the associated displacements are given by

$$\begin{aligned} u_1^S = {} & \frac{K_I}{4\mu}\sqrt{\frac{r}{2\pi}}\left[(2\kappa - 1)\cos\frac{\theta}{2} - \cos\frac{3\theta}{2}\right] \\ & + \frac{K_{II}}{4\mu}\sqrt{\frac{r}{2\pi}}\left[(2\kappa + 3)\sin\frac{\theta}{2} + \sin\frac{3\theta}{2}\right] \end{aligned} \tag{16}$$

and

$$\begin{aligned} u_2^S = {} & \frac{K_I}{4\mu}\sqrt{\frac{r}{2\pi}}\left[(2\kappa + 1)\sin\frac{\theta}{2} - \sin\frac{3\theta}{2}\right] \\ & + \frac{K_{II}}{4\mu}\sqrt{\frac{r}{2\pi}}\left[(2\kappa - 3)\cos\frac{\theta}{2} + \cos\frac{3\theta}{2}\right], \end{aligned} \tag{17}$$

where K_I and K_{II} are the SIFs respectively of the opening and sliding modes; the constant $\kappa = 3 - 4\nu$ is defined for plain strain and $\kappa = (3 - \nu)/(1 + \nu)$ for plain stress, where ν is Poisson's ratio; the constant μ is the shear modulus. The polar coordinate reference system (r, θ) is centred at the crack tip, such that $\theta = 0$ is the crack axis, ahead of the crack tip, as represented in Figure 1. Notice that the stress field is of the order $r^{-1/2}$ which becomes singular as r tends to zero. This behaviour can be clearly seen in Figure 2, which represents the stress field, in a neighbourhood of the tip of a horizontal crack, with $K_I = 1$ and $K_{II} = 0$. Notice also that the displacement field does not include rigid-body terms, hence leading to null components at the crack tip.

For general edge and internal piecewise-flat multi-cracked finite plates, under mixed-mode deformation, Caicedo and Portela (2015) have demonstrated that the first term of William's eigenexpansion, derived for a semi-infinite edge crack, can also be used to represent the elastic field, in a crack tip neighbourhood, where the singular behaviour of the stress field is dominant.

The singular stress field, defined in Equations (13)–(15), is used to define the traction components at a boundary point as

$$\mathbf{t}^S = \begin{bmatrix} t_1^S \\ t_2^S \end{bmatrix} = \begin{bmatrix} \sigma_{11}^S & \sigma_{21}^S \\ \sigma_{12}^S & \sigma_{22}^S \end{bmatrix} \begin{bmatrix} n_1 \\ n_2 \end{bmatrix} = \begin{bmatrix} g_{11} & g_{12} \\ g_{21} & g_{22} \end{bmatrix} \begin{bmatrix} K_I \\ K_{II} \end{bmatrix}, \tag{18}$$

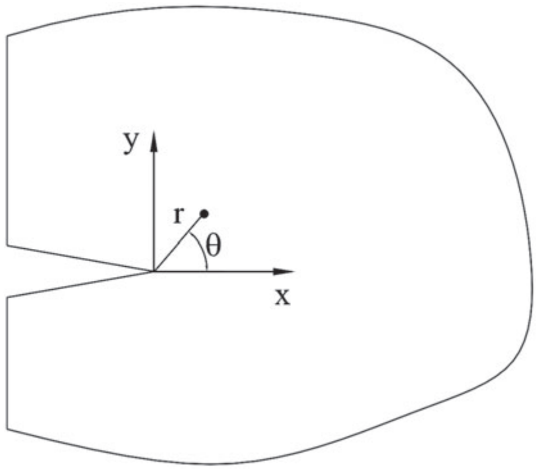

Figure 1. Reference system for Williams' singular particular solution.

where n_i denotes the ith component of the unit outward normal to the boundary and the functions $g_{ij} = g_{ij}(r^{-1/2}, \theta)$ have been introduced for a convenient short-handed notation of Equations (13)–(15).

Similarly, the displacement field, Equations (16) and (17), can be defined in a vector form as

$$\mathbf{u}^S = \begin{bmatrix} u_1^S \\ u_2^S \end{bmatrix} = \begin{bmatrix} f_{11} \; f_{12} \\ f_{21} \; f_{22} \end{bmatrix} \begin{bmatrix} K_I \\ K_{II} \end{bmatrix}, \tag{19}$$

where the functions $f_{ij} = f_{ij}(r^{1/2}, \theta)$ are a short-handed notation of Equations (16)–(17).

5. Finite element analysis

Since a formal solution of the regularised elastic model, defined by the field Equations (8)–(10), with boundary conditions (11) and (12), is generally not available for practical problems, discretisation must be used in order to obtain an approximate numerical solution.

The FEM is possibly the most popular discretisation model available in engineering, see Zienkiewicz (1977). When the method is based on weighted residuals, the starting point of its formulation is the weak form

$$\int_\Omega \sigma^{R^T} \delta\varepsilon^R \, \mathrm{d}\Omega = \int_{\Gamma_t} \left(\bar{\mathbf{t}} - \mathbf{t}^S\right)^T \delta\mathbf{u}^R \, \mathrm{d}\Gamma, \tag{20}$$

in which the virtual displacements $\delta\mathbf{u}^R$, represent arbitrary weighting functions of Galerkin's approximation. The details of this weak-form derivation can be seen in Portela and Charafi (2002).

Computation of the weak form (20) is based on the domain and boundary discretisation with a FEM, where the continuous domain Ω is replaced by the assembled finite elements Ω^e and the continuous boundary Γ is replaced by the

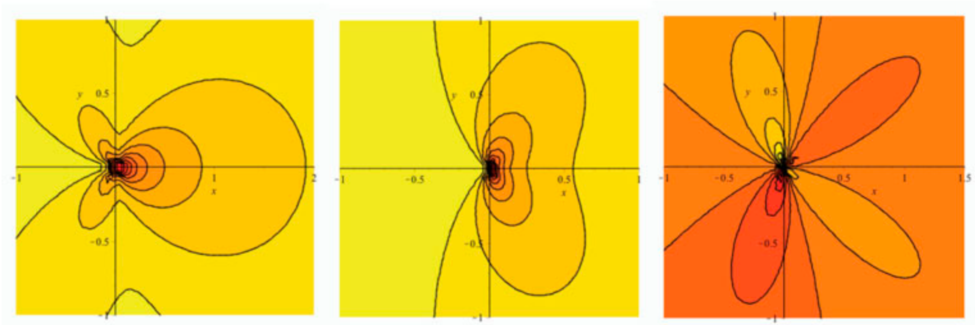

(a) σ^S_{11}. (b) σ^S_{22}. (c) σ^S_{12}.

Figure 2. Williams' stress field, in a neighbourhood of the tip of a horizontal crack, with $K_I = 1$ and $K_{II} = 0$.

assembled finite elements Γ^e. Through this process of discretisation, the FEM ultimately reduces the infinite number of degrees of freedom of the continuum problem to a finite number of unknowns defined at element nodes.

5.1. Element equations

Consider the discretisation of the domain Ω into finite elements Ω^e which leads to the discretisation of the boundary Γ into finite elements Γ^e. This discretisation process is usually represented by

$$\Omega = \sum_e \Omega^e \quad \text{and} \quad \Gamma = \sum_e \Gamma^e.$$

In each finite element Ω^e a local direct approximation is define as

$$\mathbf{u}^R = \mathbf{N}\,\mathbf{u}^e, \tag{21}$$

where $\mathbf{u}^e$ denotes the element degrees of freedom which are the nodal displacements and $\mathbf{N}$ denotes the element shape functions assigned to the degrees of freedom of the element. The assumed displacement approximation implies that the consequent approximation of strains and stresses is defined also in terms of the nodal displacements, respectively as

$$\varepsilon^R = \mathbf{L}\,\mathbf{u}^R = \mathbf{L}\,\mathbf{N}\,\mathbf{u}^e = \mathbf{B}\,\mathbf{u}^e \tag{22}$$

and

$$\sigma^R = \mathbf{D}\,\varepsilon^R = \mathbf{D}\,\mathbf{B}\,\mathbf{u}^e. \tag{23}$$

Virtual displacements and virtual strains are defined in terms of the nodal virtual displacements $\delta\mathbf{u}^e$, respectively as

$$\delta\mathbf{u}^R = \mathbf{N}\,\delta\mathbf{u}^e \tag{24}$$

and

$$\delta\varepsilon^R = \mathbf{L}\,\delta\mathbf{u}^R = \mathbf{L}\,\mathbf{N}\,\delta\mathbf{u}^e = \mathbf{B}\,\delta\mathbf{u}^e. \tag{25}$$

When these approximations are introduced in the weak form (20), the following equation is obtained

$$\delta\mathbf{u}^{eT}\left\{\int_{\Omega^e}\mathbf{B}^T\mathbf{D}\mathbf{B}\,\mathrm{d}\Omega\;\mathbf{u}^e - \int_{\Gamma_t^e}\mathbf{N}^T(\bar{\mathbf{t}}-\mathbf{t}^S)\,\mathrm{d}\Gamma\right\} = 0. \tag{26}$$

Since virtual displacements $\delta\mathbf{u}^e$ are arbitrary, the equation

$$\mathbf{K}^e\,\mathbf{u}^e = \mathbf{P}^e - \mathbf{Q}^e \tag{27}$$

holds for each finite element, where

$$\mathbf{K}^e = \int_{\Omega^e} \mathbf{B}^T \mathbf{D} \mathbf{B} \, \mathrm{d}\Omega \tag{28}$$

is the element stiffness matrix and the vectors

$$\mathbf{P}^e = \int_{\Gamma_t^e} \mathbf{N}^T \, \bar{\mathbf{t}} \, \mathrm{d}\Gamma \tag{29}$$

and

$$\mathbf{Q}^e = \int_{\Gamma_t^e} \mathbf{N}^T \mathbf{t}^S \, \mathrm{d}\Gamma \tag{30}$$

define the element load vector which leads to equivalent nodal forces. When the singular tractions, defined in Equations (18), are introduced in the element load vector $\mathbf{Q}^e$, Equations (30) can be written as

$$\mathbf{Q}^e = \int_{\Gamma_t^e} \mathbf{N}^T \begin{bmatrix} g_{11} & g_{12} \\ g_{21} & g_{22} \end{bmatrix} \begin{bmatrix} K_I \\ K_{II} \end{bmatrix} \mathrm{d}\Gamma = \mathbf{G}^e \begin{bmatrix} K_I \\ K_{II} \end{bmatrix} = \mathbf{G}^e \, \mathbf{k}, \tag{31}$$

in which the matrix $\mathbf{G}^e$ has 2 columns and as many rows as the vector $\mathbf{u}^e$ of the element unknowns, while the vector $\mathbf{k}$ denotes the SIFs K_I and K_{II}. As the SIFs are not known at this stage of a general problem, they become additional primary unknowns. Hence, the element Equations (21) can be rewritten as

$$\mathbf{K}^e \, \mathbf{u}^e = \mathbf{P}^e - \mathbf{G}^e \, \mathbf{k} \tag{32}$$

and rearranged as

$$\begin{bmatrix} \mathbf{K}^e & \mathbf{G}^e \end{bmatrix} \begin{bmatrix} \mathbf{u}^e \\ \mathbf{k} \end{bmatrix} = \begin{bmatrix} \mathbf{P}^e \end{bmatrix}, \tag{33}$$

in order to collect the unknowns in the left hand side of the equations.

5.2. Element assembly

The assembly of the element matrices $\mathbf{K}^e$, $\mathbf{G}^e$ and $\mathbf{P}^e$, processed in accordance with the respective element incidences, generates the corresponding global matrices $\mathbf{K}$, $\mathbf{G}$ and $\mathbf{P}$ for the whole FEM. This operation, supported by the reduced compatibility condition, is usually represented, respectively as

$$\mathbf{K} = \sum_e \mathbf{K}^e, \quad \mathbf{G} = \sum_e \mathbf{G}^e \quad \text{and} \quad \mathbf{P} = \sum_e \mathbf{P}^e.$$

Through the assembly process, the element Equations (33) lead to the global FEM equations represented by

$$\begin{bmatrix} \mathbf{K} & \mathbf{G} \end{bmatrix} \begin{bmatrix} \mathbf{u}^R \\ \mathbf{k} \end{bmatrix} = \begin{bmatrix} \mathbf{P} \end{bmatrix}. \tag{34}$$

Note that these global equations introduce two additional unknowns, the SIFs K_I and K_{II}, represented in vector $\mathbf{k}$. Consequently, in order to have a well-posed problem with a unique solution, it is necessary to specify two additional constraints that is one for each deformation mode included in the analysis. These additional constraints will be specified in two additional bottom rows in Equations (34).

5.3. Additional constraints

Additional constraints can be specified in several different ways. However, they must enforce the cancellation of the singularity, in the regularised field, introduced through Equations (6) and (7). The most obvious conditions that do reflect this consideration are that, either the regular displacement field, or the regular stress field is cancelled out at the crack tip, that is

$$u_i^R = 0 \;\Rightarrow\; u_i = u_i^S, \tag{35}$$

or

$$\sigma_{ij}^R = 0 \;\Rightarrow\; \sigma_{ij} = \sigma_{ij}^S \tag{36}$$

which ensure that the original elastic field is singular at the crack tip.

Since the problem is formulated in terms of the regularised displacement components u_i^R, the additional constraints must be defined in terms of the nodal components included in the vector of the unknowns $\mathbf{u}^R$, in order to be effective. Hence, to fulfill this requirement, conditions (35) can be used as additional constraints. However, since the displacement components of the singular elastic field, Equations (16) and (17), do not include rigid-body terms, the use of conditions (35) leads to null displacement components of the original problem at the crack tip which can overconstrain the original problem. Therefore, the use of conditions (35), as the additional constraints to be specified in Equations (34), is ruled out.

On the other hand, conditions (36) are not defined in terms of the nodal components of the regularised displacements u_i^R included in the vector of the unknowns $\mathbf{u}^R$ and, therefore, they cannot be used simply as they are, in order to effectively define the additional constraints required by Equations (34). To overcome this difficulty, conditions (36) are first rewritten in terms of the respective traction components, defined at the crack tip, as

$$t_j^R = \sigma_{ij}^R n_i = 0 \;\Rightarrow\; t_j = t_j^S, \tag{37}$$

where n_i represent the outward unit normal components to the crack faces. Now consider the patch of finite elements that share the crack tip node. When these elements are submitted to an arbitrary rigid-body displacement, conditions (37) are exactly satisfied. This rigid-body displacement can be easily implemented through a set of multi-constraint conditions, specifying identical displacements for the crack tip node and each node of the referred patch of finite elements. Although this procedure is effective, because the multi-constraint conditions are defined in terms of the nodal components of the regularised displacements u_i^R included in the vector of the unknowns $\mathbf{u}^R$, it can affect the solution accuracy. This is a drawback that can easily be overcome through a mesh refinement around the crack tip, in order to minimise the extension where the multi-constraint of the rigid-body displacement is applied.

For the sake of simplicity, the strategy adopted in this paper, to define the additional constraints required in Equations (34), to fulfil the conditions of a well-posed problem with a unique solution in the regularisation process, considers identical displacements only for the crack tip node and its neighbour node just ahead of the crack tip, which minimises the referred drawback of the rigid-body condition applied to all the nodes of the finite elements that share the crack tip node. Thus, the additional constraints that must be specified in Equations (34) are finally defined as

$$\mathbf{u}_r^R = \mathbf{u}_s^R, \tag{38}$$

in which r represents the crack tip node and s represents the node ahead of the crack tip; $\mathbf{u}_r^R$ represents the displacement components of the crack tip node, while $\mathbf{u}_s^R$ represents the displacement components of the node ahead of the crack tip.

The implementation of this strategy is quite simple. Consider, for instance, that the crack tip node numbering is r which leads to the assignment of the degrees of freedom $2r - 1$ and $2r$ to the node. Consider also that the numbering of the neighbour node ahead of the crack tip is s, which now leads to the assignment of the degrees of freedom $2s - 1$ and $2s$ to this node. Under this assumption, the additional constraints (38) can be included in the analysis through a simple modification of the global system of Equations (34) as

$$\begin{bmatrix} \mathbf{K} & \mathbf{G} \\ \mathbf{C} & \mathbf{0} \end{bmatrix} \begin{bmatrix} \mathbf{u}^R \\ \mathbf{k} \end{bmatrix} = \begin{bmatrix} \mathbf{P} \\ \mathbf{0} \end{bmatrix}, \tag{39}$$

in which matrix $\mathbf{C}$ is given by

$$\mathbf{C} = \begin{bmatrix} 0 & \cdots & 1 & 0 & \cdots & -1 & 0 & \cdots & 0 \\ 0 & \cdots & 0 & 1 & \cdots & 0 & -1 & \cdots & 0 \end{bmatrix}, \tag{40}$$

where, for the numbering assumption considered, the identity terms are in columns $2r - 1$ and $2r$, to be multiplied by the corresponding terms of $\mathbf{u}_r^R$ and the -1 terms are in columns $2s - 1$ and $2s$, to be multiplied by the corresponding terms of $\mathbf{u}_s^R$.

5.4. Displacement boundary conditions

As a domain method, the finite element model satisfies exactly some of the boundary conditions which therefore generate trivial residuals that are not included in the weighted residual equation. This is the case of the essential boundary conditions (11) that were not included in the weighted residual Equation (20) which led to the system of algebraic Equations (39). Consequently, this system of equations must be modified in order that its solution satisfies the essential boundary conditions.

There are several procedures of introducing the essential boundary conditions in the system of equations, see Bath and Wilson (1976). To use the simplest of these methods, consider that the node number i, with assigned degrees of freedom $2i-1$ and $2i$, has constrained displacements given by the essential boundary conditions (11) as

$$\mathbf{u}^R = \overline{\mathbf{u}} - \mathbf{u}^S \tag{41}$$

that is

$$\begin{bmatrix} u^R_{2i-1} \\ u^R_{2i} \end{bmatrix} = \begin{bmatrix} \overline{u}_{2i-1} \\ \overline{u}_{2i} \end{bmatrix} - \begin{bmatrix} f_{11} \; f_{12} \\ f_{21} \; f_{22} \end{bmatrix} \begin{bmatrix} K_I \\ K_{II} \end{bmatrix}. \tag{42}$$

The simplest method is carried out in four steps. In the first step, the known nodal values of the boundary condition, respectively $\overline{u}_{2i-1}$ and $\overline{u}_{2i}$, are multiplied by the respective columns $2i-1$ and $2i$ of the matrix $\mathbf{K}$ and the result is added to the right hand side $\mathbf{P}$, in Equation (39). In the second step, the rows $2i-1$ and $2i$ as well as the columns $2i-1$ and $2i$ of the matrix $\mathbf{K}$ are filled in with zeros, while the respective diagonal terms are replaced by the unit. In the third step, the corresponding rows of the right hand side, respectively, P_{2i-1} and P_{2i} are replaced by the known nodal values, respectively, $\overline{u}_{2i-1}$ and $\overline{u}_{2i}$. Eventually, the rows $2i-1$ and $2i$ of the matrix $\mathbf{G}$ are replaced, respectively, by $[f_{11} \; f_{12}]$ and $[f_{21} \; f_{22}]$. Now, the rows $2i-1$ and $2i$ of the system of equations are given by

$$\begin{bmatrix} u^R_{2i-1} \\ u^R_{2i} \end{bmatrix} + \begin{bmatrix} f_{11} \; f_{12} \\ f_{21} \; f_{22} \end{bmatrix} \begin{bmatrix} K_I \\ K_{II} \end{bmatrix} = \begin{bmatrix} \overline{u}_{2i-1} \\ \overline{u}_{2i} \end{bmatrix}. \tag{43}$$

Alternatively, the method of Lagrange multipliers, see Felippa (2013), can be used to introduce the essential boundary conditions in the system of equations. In this case, the weighted-residual weak form (20) is expanded to include the essential boundary conditions (11) through Lagrange multipliers λ, as

$$\int_\Omega {\sigma^R}^T \delta\varepsilon^R \, d\Omega = \int_{\Gamma_t} (\overline{\mathbf{t}} - \mathbf{t}^S)^T \delta\mathbf{u}^R \, d\Gamma + \int_{\Gamma_u} (\mathbf{u}^R - \overline{\mathbf{u}} + \mathbf{u}^S)^T \delta\lambda \, d\Gamma + \int_{\Gamma_u} \lambda^T \delta\mathbf{u}^R \, d\Gamma, \tag{44}$$

in which $\delta\lambda$ represent arbitrary variations of Lagrange multipliers. This extended weak form generates the element equations

$$\begin{bmatrix} \mathbf{K}^e & \mathbf{G}^e & {\mathbf{A}^e}^T \\ \mathbf{A}^e & \mathbf{F}^e & \mathbf{0} \end{bmatrix} \begin{bmatrix} \mathbf{u}^e \\ \mathbf{k} \\ \lambda \end{bmatrix} = \begin{bmatrix} \mathbf{P}^e \\ \mathbf{V}^e \end{bmatrix}, \tag{45}$$

in which

$$\mathbf{A}^e = \int_{\Gamma_u^e} \mathbf{N}^T \, \mathrm{d}\Gamma, \tag{46}$$

$$\mathbf{V}^e = \int_{\Gamma_u^e} \mathbf{N}^T \overline{\mathbf{u}} \, \mathrm{d}\Gamma, \tag{47}$$

and, using Equations (19)

$$\mathbf{F}^e = \int_{\Gamma_u^e} \mathbf{N}^T \begin{bmatrix} f_{11} & f_{12} \\ f_{21} & f_{22} \end{bmatrix} \mathrm{d}\Gamma. \tag{48}$$

After the assembly of the element equations and the introduction of the additional constraints (38), the extended weak form (44) eventually leads to the global system of equations

$$\begin{bmatrix} \mathbf{K} & \mathbf{G} & \mathbf{A}^T \\ \mathbf{C} & \mathbf{0} & \mathbf{0} \\ \mathbf{A} & \mathbf{F} & \mathbf{0} \end{bmatrix} \begin{bmatrix} \mathbf{u}^R \\ \mathbf{k} \\ \lambda \end{bmatrix} = \begin{bmatrix} \mathbf{P} \\ \mathbf{0} \\ \mathbf{V} \end{bmatrix} \tag{49}$$

that can be solved.

6. Numerical results

This paper is concerned with the direct computation of SIFs in the FEM, through the crack tip singularity subtraction, to provide an efficient and accurate way of analysing the deformation of homogeneous cracked plates.

A computer code that implements this new formulation, with constant-strain triangular finite elements with exact integration, was developed and used to solve some numerical examples which include two different cases of edge-cracked finite plates, respectively under opening mode and sliding-mode loading. The results obtained clearly demonstrate the accuracy and reliability of this formulation.

6.1. Edge-cracked plate under opening-mode loading

Consider a square plate, with a single crack normal to one edge, as represented in Figure 3. The crack length is denoted by a, the width of the plate is denoted by w and the height by $h = w/2$. The crack position is defined in Cartesian coordinates by $0 \leq x \leq a$ and $y = 0$. The plate is subjected to the action of a uniform traction $\bar{\mathbf{t}} = \sigma$, acting in a direction perpendicular to the crack and applied symmetrically at the ends which corresponds to an opening-mode loading. Results have been obtained for the cases in which $h/w = .5$, in order to be compared with the highly accurate values published by Civelek and Erdogan (1982). Five cases were considered, with $a/w = .2, .3, .4, .5$ and $.6$, respectively. A convergence study, of the stress intensity factors, was carried out with three different meshes; convergence was achieved, for all the five cases of crack-length

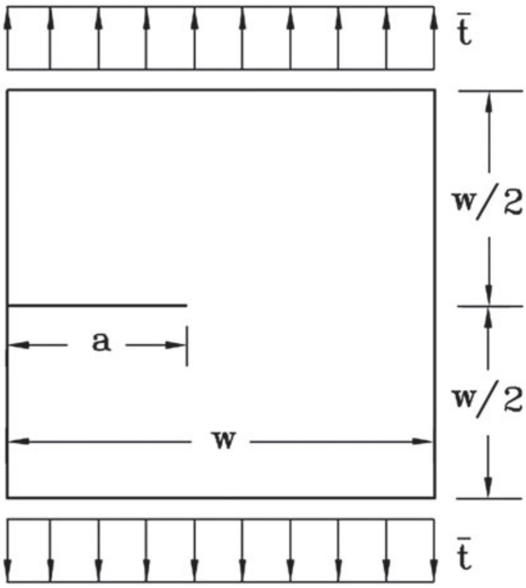

Figure 3. Square plate with a single edge crack under opening-mode loading ($h/w = .5$).

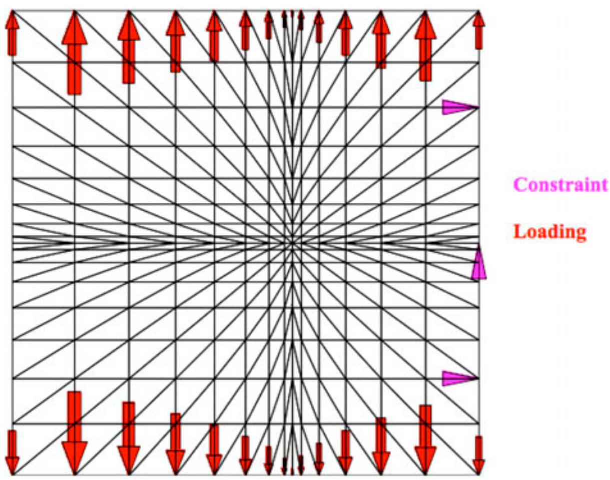

Figure 4. Finite element mesh and the boundary conditions used for the case $a/w = .6$ under opening-mode loading ($h/w = .5$).

considered, with a mesh of 576 finite elements, in which the discretisation was refined around the tip.

The results obtained with this FEM are presented in Table 1 and show a high level of accuracy when compared with those of Civelek and Erdogan (1982). Also, FEM results compare quite well with the results obtained from the J-integral technique in the dual boundary element method (J-DBEM) which is considered a highly accurate technique, (see Portela & Aliabadi, 1993). The discrepancies obtained for small crack lengths are very difficult to overcome with

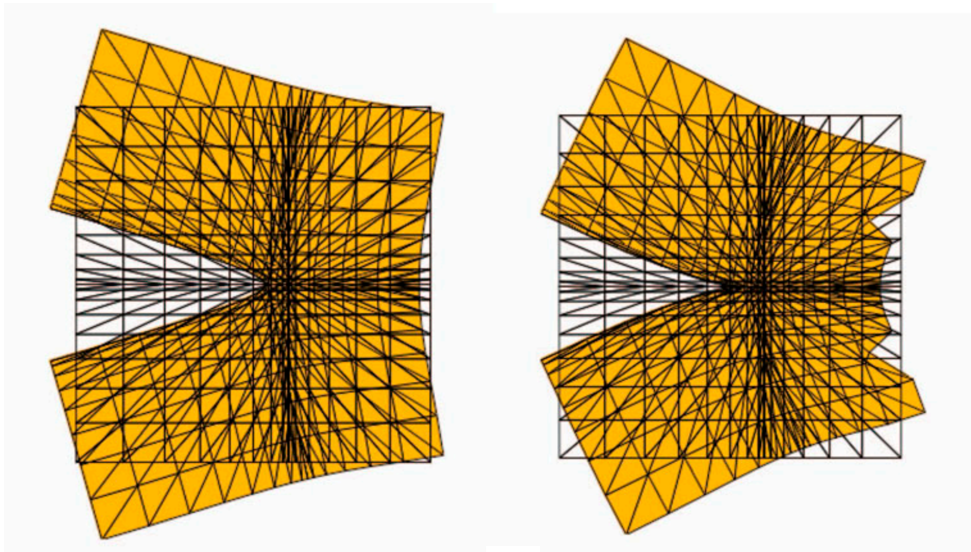

(a) Original field $u_i = u_i^R + u_i^S$.

(b) Regularized field $u_i^R = u_i - u_i^S$.

Figure 5. Initial and deformed finite element meshes for the case $a/w = .6$ under opening-mode loading.

Table 1. Stress intensity factors for a single edge crack in a square plate under opening-mode loading ($h/w = .5$).

	$K_I/(\bar{\mathbf{t}}\sqrt{\pi a})$			% Error	
a/w	FEM	J-DBEM Portela and Aliabadi (1993)	Reference Civelek and Erdogan (1982)	FEM	J-DBEM
.2	1.454	1.495	1.488	.023	.005
.3	1.825	1.858	1.848	.012	.005
.4	2.311	2.338	2.324	.006	.006
.5	3.014	3.028	3.010	.001	.006
.6	4.147	4.184	4.152	.001	.008

Notes: FEM represents the values obtained in this paper, while J-DBEM Portela and Aliabadi (1993) represents the corresponding values obtained with the J-integral in the dual boundary element method. Percentage errors are computed from the accurate values of reference (Civelek & Erdogan, 1982).

Table 2. Stress intensity factors for a single edge crack in a square plate under sliding-mode loading ($h/w = .5$).

	$K_{II}/(\bar{\mathbf{t}}\sqrt{\pi a})$		
a/w	FEM	J-DBEM Portela and Aliabadi (1993)	% Error
.2	.437	.435	.005
.3	.356	.358	.006
.4	.303	.304	.003
.5	.263	.262	.004
.6	.223	.223	.000

Notes: FEM represents the values obtained in this paper, while J-DBEM Portela and Aliabadi (1993) represents the corresponding values obtained with the J-integral in the dual boundary element method. Percentage errors are computed from the accurate values of J-DBEM.

constant-strain triangular elements used in FEM. It is important to note that the stress intensity factors of the sliding deformation mode are always below 10^{-7} as expected, since this is mainly an opening deformation mode crack problem. Figure 4 shows the FEM and the boundary conditions for the case $a/w = .6$. Figure 5 shows the initial and deformed FEMes of both the original and regularised elastic fields, for the case $a/w = .6$. Notice the difference of the opened crack surfaces in both cases of the original and regularised elastic fields. Notice also the influence of the boundary conditions (41) in the regularised displacement field.

6.2. *Edge-cracked plate under sliding-mode loading*

Consider a square plate, with a single crack normal to one edge, as represented in Figure 6. The crack length is denoted by a and the ratio between the height and the width of the plate is given by $h/w = .5$. The plate is loaded with a uniform traction $\bar{\mathbf{t}} = \sigma$, acting now in a direction parallel to the crack and applied anti-symmetrically at the sides which corresponds to a sliding-mode loading. This is a very difficult case, for which there are no published benchmark results, as far as the authors knowledge is concerned. Therefore, results have been obtained with the present formulation, in order to be compared with those obtained by J-DBEM, using the software (Portela & Aliabadi, 1993). This combination of the dual boundary element method with the J-integral technique is an extremely-

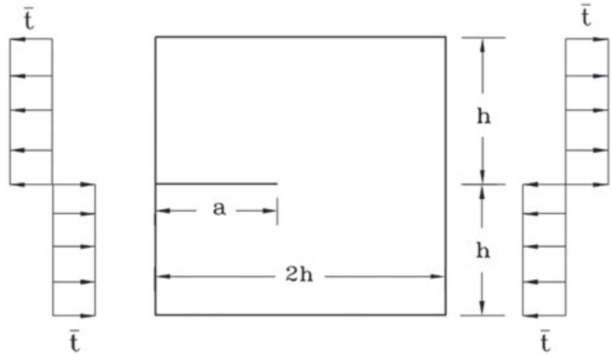

Figure 6. Square plate with a single edge crack under sliding-mode loading ($w = 2h$).

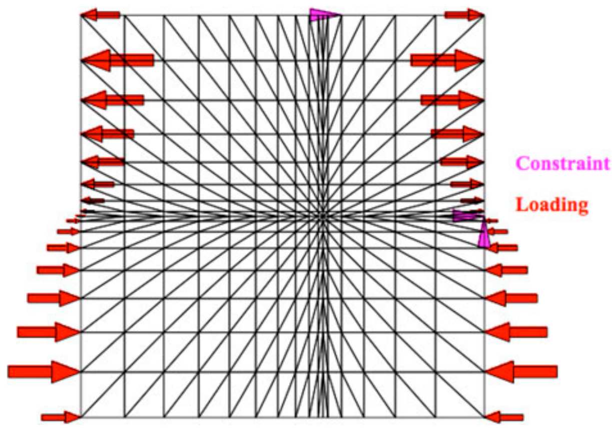

Figure 7. Finite element mesh and the boundary conditions used for the case $a/w = .6$ under sliding-mode loading ($h/w = .5$).

accurate tool because it uses the elastic field computed at internal points which is a highly accurate operation in the BEM due to the presence of the fundamental solutions. Five cases were considered, with corresponding $a/w = .2, .3, .4, .5$ and .6. A convergence study, of the stress intensity factors, was carried out with three different meshes; convergence was achieved, for all the five cases of crack-length considered, with a mesh of 512 finite elements, in which the discretisation was refined around the tip.

The results obtained with this FEM, presented in Table 2 are remarkably accurate; FEM results match those obtained with J-DBEM (Portela & Aliabadi, 1993) within two decimal places. It is important to note that the stress intensity factors of the opening deformation mode are always below 10^{-3}, since this is mainly a sliding deformation mode crack problem. Figure 7 shows the FEM and the boundary conditions used for the case $a/w = .6$. The initial and deformed finite element meshes of both the original and regularised elastic fields, for the

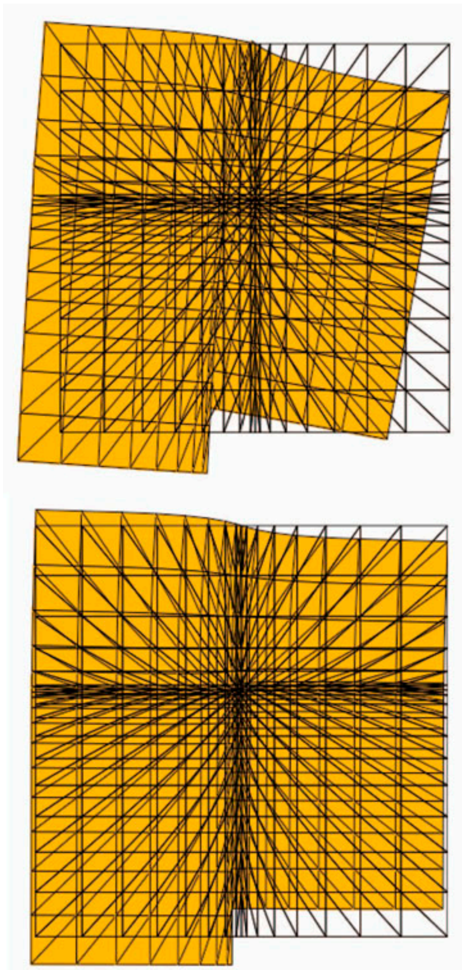

(a) Original field $u_i = u_i^R + u_i^S$.

(b) Regularized field $u_i^R = u_i - u_i^S$.

Figure 8. Initial and deformed finite element meshes for the case $a/W = .6$ under sliding-mode loading.

case $a/w = .6$, are shown in Figure 8, where the influence of the boundary conditions (41) in the regularised displacement field can be seen.

7. Conclusions

This paper is concerned with the direct computation of SIFs, to provide an efficient and accurate way of analysing the deformation of cracked plates with the FEM. This feature that is the direct computation of SIFs in the finite element analysis, is a natural consequence of a regularisation procedure that uses a singular particular solution of the crack problem, to introduce the SIFs as additional primary unknowns in the finite element analysis. In this paper, the singular term of Williams' eigenexpansion is the particular solution used in the regularisation process of any crack problem.

After a thorough review of the most important approaches that have been devised to overcome the well-known difficulties that arise in the numerical modelling of elastic fields with singularities, in the standard FEM, in the XFEM, in the dual BEM and in mesh-free methods, it was concluded that there is room for a radically different approach, of the ones adopted by these methods, which completely removes the crack tip singularity, before the finite element analysis of the regularised elastic field is carried out, leading conveniently to no convergence difficulties with smooth and highly accurate solutions.

The reliability of this robust modelling strategy, that regularises the elastic problem through the crack tip singularity subtraction, before its solution with the FEM, was assessed with the analysis of the edge-crack plate under opening-mode and sliding-mode loading; the results obtained clearly demonstrate the excellent accuracy of this new formulation of the FEM.

Despite the highly accurate results obtained in this paper, it is necessary to carry out further research, in order to improve the efficiency of the singularity-subtraction modelling strategy of this paper. Effectively, since the finite element analysis is carried out on a regularised elastic problem, it does not require the use of refined meshes around the crack tip, because the singularity was already removed in the regularisation process. However, the lack of rigid-body displacement terms in Williams' eigenexpansion does not allow using the additional constraints (35), to fulfil the conditions of a well-posed problem with a unique solution in the regularisation process, because the crack tip displacement becomes overconstrained, and therefore, the additional constraints (36) must be used instead. Hence, considering the additional constraints (38), which represent a rigid-body displacement constraint ahead of the crack tip that implicitly satisfies the additional constraints (36), requires the use of refined meshes around the crack tip, in order to minimise the extension where the rigid-body displacement constraint is applied and consequently obtain accurate results. This is a drawback of the present formulation that is a direct consequence of the lack of rigid-body displacement components in Williams' eigenexpansion. Therefore, aiming highly accurate results, obtained with a finite element analysis carried out on regular meshes, instead of refined ones, it is necessary to consider the alternative additional constraints (35) which in general is not possible, without including in Williams' eigenexpansion additional terms to account for the possibility of describing rigid-body displacements of the crack tip. This enhancement is not in the scope of the paper and is a matter for further research work that eventually will lead to accurate results, with an even more efficient singularity-subtraction modelling strategy in the FEM.

The modelling strategy presented in this paper, concerned with the direct computation of SIFs, can be easily extended to the analysis of 3D crack problems. Effectively, whenever the crack tip asymptotic elastic field is available, it can be used in the regularisation of the elastic field, as in the case of 2D crack problems. The 3D stress field ahead of a partially through the thickness crack was investigated analytically by Folias (1975), who derived an asymptotic solution valid at the base of a partially through the thickness crack, similar to Williams' expansion, based in 2D considerations. In this context see also the works of Bethem (1977) and Shivakumar and Raju (1990) for cylindrical and vertex singularities.

The direct computation of SIFs, with the modelling strategy presented in this paper, can be easily implemented in XFEM. Effectively, it is well-known that in XFEM, the solution accuracy of the local fields around a crack tip is a direct consequence of the choice carried out for the enrichment functions that define *apriori*-knowledge of the solution. The closer these enrichment functions are to the exact asymptotic fields, the better is the solution accuracy. Modern XFEM formulations rely on truncated Williams' expansion that is dedicated to straight cracks only. In the general case of non-straight cracks, the singular enrichment zone must be defined on the scale on which the crack can be considered straight. Therefore, the finite-element mesh must be fine enough to fit with this scale, which is a drawback of the current XFEM. However, this drawback can be easily overcome through the implementation of the direct computation of SIFs, with the singularity subtraction technique presented in this paper, to regularise the elastic field prior solution and consequently simplify the XFEM enrichment process over a regular mesh.

Acknowledgements

The first author acknowledges the program *PECC – Pós-Graduação em Estruturas e Construção Civil*, Department of Civil Engineering, Faculty of Technology, University of Brasília. He also acknowledges *CAPES – Coordenação de Aperfeiçoamento de Pessoal de Nível Superior* for his Master scholarship.

Disclosure statement

No potential conflict of interest was reported by the authors.

ORCID

A. Portela http://orcid.org/0000-0003-1342-1480

References

Akhondzadeh, Sh, Khoei, A. R., & Broumand, P. (2017). An efficient enrichment strategy for modeling stress singularities in isotropic composite materials with X-FEM technique. *Engineering Fracture Mechanics, 169*, 201–225.

Aliabadi, M. H. (1987). *An enhanced boundary element method for determining fracture parameters*. In Proceedings 4th International Conference on Numerical Methods in Fracture Mechanics, 27–39. San Antonio, TX: Pineridge Press.

Aliabadi, M. H., Rooke, D. P., & Cartwright, D. J. (1987). An improved boundary element formulation for calculating stress intensity factors: Application to aerospace structures. *Journal of Strain Analysis, 22*, 1–5.

Barsoum, R. S. (1976). On the use of isoparametric finite elements in linear fracture mechanics. *International Journal for Numerical Methods in Engineering, 10*, 25–37.

Bath, K. J., & Wilson, E. L. (1976). *Numerical methods in finite element analysis*. New Jersey, NJ: Prentice Hall.

Belytschko, T., & Black, T. (1999). Elastic crack growth in finite elements with minimal remeshing. *International Journal for Numerical Methods in Engineering, 45*, 601–620.

Belytschko, T., Krongauz, Y., & Organ, D. (1996). Meshless methods: An overview and recent developments. *Computer Methods in Applied Mechanics and Engineering, 139*, 3–47.

Bethem, J. P. (1977). State of stress at vertex of a quarter-infinite crack in a half-space. *International Journal of Solids and Structures, 13*, 479–492.

Blandford, G. E., Ingraffea, A. R., & Liggett, J. A. (1981). Two-dimensional stress intensity factor computations using the boundary element method. *International Journal for Numerical Methods in Engineering, 17*, 387–404.

Bordas, S., & Duflot, M. (2007). Derivative recovery and a posteriori error estimate for extended finite elements. *Computer Methods in Applied Mechanics and Engineering, 196*, 3381–3399.

Bordas, S., Duflot, M., & Le, P. (2008). A simple error estimator for extended finite elements. *Communications in Numerical Methods in Engineering, 24*, 961–971.

Bordas, S., Rabczuk, T., & Zi, G. (2008). Three-dimensional crack initiation, propagation, branching and junction in non-linear materials by an extended meshfree method without asymptotic enrichment. *Engineering Fracture Mechanics, 75*, 943–960.

Brahtz, J. H. A. (1933). Stress distribution in a reentrant corner. *Transactions of the American Society of Mechanical Engineers, 55*, 31–37.

Caicedo, J., & Portela, A. (2015). Cracked plate analysis with the dual boundary element method and Williams' eigen expansion. *Journal of Engineering Analysis with Boundary Elements, 52*, 16–23.

Carpinteri, A., Ferro, G., & Ventura, G. (2003). The partition of unity quadrature in element-free crack modeling. *Computers and Structures, 81*, 1783–1794.

Civelek, M. B., & Erdogan, F. (1982). *International Journal of Fracture, 19*, 139–159. Retrieved from https://link.springer.com/article/10.1007/BF00016570

Cruse, T. A., & Wilson, R. B. (1977). Boundary integral equation method for elastic fracture mechanics analysis, AFOSR-TR-780355, Pratt and Whitney Aircraft Group, Hartford, Connecticut.

Dong, L., & Atluri, S. N. (2013). Fracture and fatigue analyses: SGBEM-FEM or XFEM? Part 1: 2D structures. *Computer Modeling in Engineering and Sciences, 90*, 91–146.

Duflot, M., & Bordas, S. (2008). A posteriori error estimation for extended finite elements by an extended global recovery. *International Journal for Numerical Methods in Engineering, 76*, 1123–1138.

Estrada, O., Rdenas, J., Bordas, S., Duflot, M., Kerfriden, P., & Giner, E. (2012). On the role of enrichment and statical admissibility of recovered fields in a posteriori error estimation for enriched finite element methods. *Engineering Computations, 29*, 814–841.

Felippa, C. A. (2013). *Introduction to finite element methods*. Boulder: University of Colorado. Retrieved from http://www.colorado.edu/engineering/cas/courses.d/IFEM.d/

Fleming, M., Chu, Y., Moran, B., & Belytschko, T. (1997). Enriched element-free Galerkin methods for crack tip fields. *International Journal for Numerical Methods in Engineering, 40*, 1483–504.

Folias, E. S. (1975). On the three-dimensinal theory of cracked plates. *Journal of Applied Mechanics, 42*, 663–674.

Gu, Y. T., & Zhang, L. C. (2008). Coupling of the meshfree and finite element methods for determination of the crack tip fields. *Engineering Fracture Mechanics, 75*, 986–1004.

Hedayati, E., & Vahedi, M. (2014). Using extended finite element method for computation of the stress intensity factor, crack growth simulation and predicting fatigue crack growth in a slant-cracked plate of 6061–T651 aluminum. *World Journal of Mechanics, 4*, 24–30.

Henshell, R. D., & Shaw, K. G. (1975). Crack tip elements are unnecessary. *International Journal for Numerical Methods in Engineering, 9*, 495–509.

Karihaloo, B. L., & Xiao, Q. Z. (2001). Accurate determination of the coefficients of elastic crack tip asymptotic field by a hybrid crack element with p-adaptivity. *Engineering Fracture Mechanics, 68*, 1609–1630.

Khoei, A. R. (2015). *Extended finite element method: Theory and applications*. London: Wiley.

Li, S., & Liu, W. K. (2002). Meshfree and particle methods and their applications. *Applied Mechanics Reviews, 54*, 1–34.

Liu, G. R., & Gu, Y. T. (2005). *An introduction to meshfree methods and their programming*. Berlin: Springer Press.

Liu, X. Y., Xiao, Q. Z., & Karihaloo, B. L. (2004). Xfem for direct evaluation of mixed mode stress intensity factors in homogeneous and bi-materials. *International Journal for Numerical Methods in Engineering, 59*, 1103–1118.

Lu, Y. Y., Belytschko, T., & Tabbara, M. (1995). Element-free Galerkin method for wave propagation and dynamic fracture. *Computer Computer Methods in Applied Mechanics and Engineering, 126*, 131–53.

Martinez, J., & Dominguez, J. (1984). On the use of quarter-point boundary elements for stress intensity factor computations. *International Journal for Numerical Methods in Engineering, 20*, 1941–1950.

Melenk, J. M., & Babuska, I. (1996). The partition of unity finite element method: Basic theory and applications. *Computer Methods in Applied Mechanics and Engineering, 139*, 289–314.

Natarajana, S., Ooi, E., Chiong, I., & Song, C. (2014). Convergence and accuracy of displacement based finite element formulations over arbitrary polygons: Laplace interpolants, strain smoothing and scaled boundary polygon formulation. *Finite Elements in Analysis and Design, 85*, 101–122.

Natarajana, S., Songa, C., & Belouettarb, S. (2014). Numerical evaluation of stress intensity factors and T-stress for interfacial cracks and cracks terminating at the interface without asymptotic enrichment. *Computer Methods in Applied Mechanics and Engineering, 279*, 86–112.

Nguyen, V. P., Rabczuk, T., Bordas, S., & Duflotd, M. (2008). Meshless methods: A review and computer implementation aspects. *Mathematics and Computers in Simulation, 79*, 763–813.

Ooi, E., Song, C., Loi, F., & Yang, Z. (2012). Polygon scaled boundary finite elements for crack propagation modelling. *International Journal for Numerical Methods in Engineering, 91*, 319–342.

Portela, A., & Aliabadi, M. H. (1993). *Crack growth analysis using boundary elements – Software*. Southampton, Boston: Computational Mechanics Publications. Press (1987).

Portela, A., Aliabadi, M. H., & Rooke, D. P. (1991). Efficient boundary element analysis of sharp notched plates. *International Journal for Numerical Methods in Engineering, 32*, 445–470.

Portela, A., Aliabadi, M. H., & Rooke, D. P. (1992). The dual boundary element method: Effective implementation for crack problems. *International Journal for Numerical Methods in Engineering, 33*, 1269–1287.

Portela, A., Aliabadi, M. H., & Rooke, D. P. (1992). Dual boundary element analysis of cracked plates: Singularity subtraction technique. *International Journal of Fracture, 55*, 17–28.

Portela, A., Aliabadi, M. H., & Rooke, D. P. (1989). *Boundary element analysis of V-notched plates*. In C. A. Brebbia, Proceedings of the fourth International Conference on Boundary Element Technology, Windsor, Canada, Southampton: Computational Mechanics Publications.

Portela, A., & Charafi, A. (2002). *Finite elements using maple – A Symbolic programming approach*. Berlin: Springer.

Prange, C., Loehnert, S., & Wriggers, P. (2012). Error estimation for crack simulations using the XFEM. *International Journal for Numerical Methods in Engineering, 91*, 1459–1474.

Rabczuk, T., & Belytschko, T. (2007). A three-dimensional large deformation meshfree method for arbitrary evolving cracks. *Computer Methods in Applied Mechanics and Engineering, 196*, 2777–2799.

Rdenas, J., Estrada, O., Tarancn, E., & Fuenmayor, F. (2008). A recovery-type error estimator for the extended finite element method based on singular+smooth stress field splitting. *International Journal for Numerical Methods in Engineering, 76*, 545–571.

Rodenas, J., Estrada, O., Diez, P., & Fuenmayor, F. (2010). Accurate recovery-based upper error bounds for the extended finite element framework. *Computer Methods in Applied Mechanics and Engineering, 199*, 2607–2621.

Shivakumar, K. N., & Raju, I. S. (1990). Treatment of singularities in cracked bodies. *International Journal of Fracture, 45*, 159–178.

Sladek, J., Sladek, V., Wunsche, M., & Zhang, C. (2009). Interface crack problems in anisotropic solids analyzed by the MLPG. *Computer Modeling in Engineering and Sciences, 54*, 223–252.

Smith, R. N. L., & Mason, J. C. (1987). A boundary element method for curved crack problems in two-dimensions. In C. A. Brebbia (Ed.), *Proceedings of Fourth International Seminar on BEM*. Berlin: Springer-Verlag.

Symm, G. T. (1963). Integral equation methods in potential theory II. *Proceedings of Royal Society, A275*, 33–46.

Tong, P., Pian, T. H. H., & Lasry, S. J. (1973). A hybrid element approach to crack problems in plane elasticity. *International Journal for Numerical Methods in Engineering, 7*, 297–308.

Wen, P. H., & Aliabadi, M. H. (2007). Applications of meshless method to fracture mechanics with enriched radial basis functions. *Durability of Structures and Health Monitoring, 3*, 107–119.

Williams, M. L. (1952). Stress singularities resulting from various boundary conditions in angular corners of plates in extension. *Journal of Applied Mechanics*, 526–528. ISSN: 0021-8936.

Xanthis, L. S., Bernal, M. J. M., & Atkinson, C. (1981). The treatment of the singularities in the calculation of stress intensity factors using the integral equation method. *Computer Methods in Applied Mechanics and Engineering, 26*, 285–304.

Xiao, Q. Z., Karihaloo, B. L., & Liu, X. Y. (2004). Direct determination of SIF and higher order terms of mixed-mode cracks by a hybrid crack element. *International Journal of Fracture, 125*, 207–225.

Zienkiewicz, O. C. (1977). *The finite element method*. New York, NY: Mc Graw-Hill.